Stability Limits and Fuel Placement in Carbureted Fuel Injection System (CFIS) Flameholder

Phase I Final Report

Reporting Period Start Date: 15 March 2007
Reporting Period End Date: 31 August 2007

PDPI: Ben T Zinn
CoPDPI: Eugene Lubarsky

Caleb N. Cross
John T. Cutright

Date Report was Issued:

30 August 2007

Account # 1606A67
P/S Fund # R8246

School of Aerospace Engineering

Georgia Institute of Technology

Atlanta, GA 30332-0150

Table of Contents

1. Abstract

A novel flameholder that makes use of a carbureted fuel injection system (CFIS) has recently been developed and tested. Initial experimentation of the CFIS flameholder was performed at the Ben T. Zinn Combustion Laboratory at Georgia Tech. Four different fuel injection configurations were tested under various operating conditions in order to determine the stability limits of the CFIS flameholder. In addition, Phase Doppler Particle Analyses (PDPA) were performed during testing of one CFIS configuration to measure fuel droplet size, velocity, and volume flux emanating from the CFIS exit channels and in the recirculation zone. All four flameholder configurations were able to operate stably only at lean afterburner equivalence ratios. Initial PDPA scans indicated a lack of fuel in the vane wake just downstream of the trailing edge. Further testing is required to properly identify the primary cause of narrow stability margins and expand stable operating conditions to include richer operation.

2. Description of Design

A schematic outlining the basic principles of the baseline CFIS flameholder configuration is shown in Figure 1. High-temperature vitiated air enters carburetor channels located within the flameholder. Fuel is then injected into the carbureted air flow just downstream of the vitiated air entrance. The fuel droplets atomize and partially vaporize due to the high velocity and high temperature of the incoming air, and the resulting fuel-rich air mixture is injected normal to or at an angle to the main air stream just upstream of the trailing edge of the flameholder.

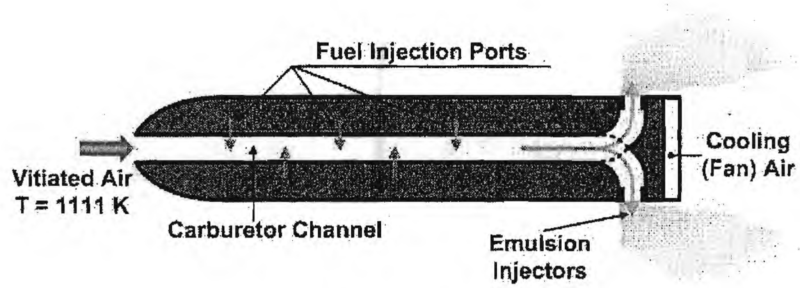

Figure 1: Conceptual Schematic of CFIS Flameholder

Figure 2 shows an exploded view of the baseline CFIS flameholder assembly. The assembled design consists of a stainless steel core, eight brass injectors, hollow leading and trailing edge hoods made from Haynes 188 alloy, and four stainless steel carburetor tubes. These tubes connect to four carburetor channels drilled within the vane core. The injectors are arranged in an impinging jet configuration (four on each side). The design allows for replacement of these injectors with cross flow injectors in order to simultaneously inject fuel directly into the air stream as well as into the carburetor channels. The opening of each carburetor channel is located one inch upstream of the vane trailing edge in order to provide injection of the two phase fuel-air mixture into the main air stream. These openings are arranged in a staggered array with two on each side of the vane. The trailing edge is hollow and is cooled by air supplied to an internal network of air ducts contained within the vane core. The assembled flameholder has overall dimensions of 8 inches by 3 inches by 1.875 inches.

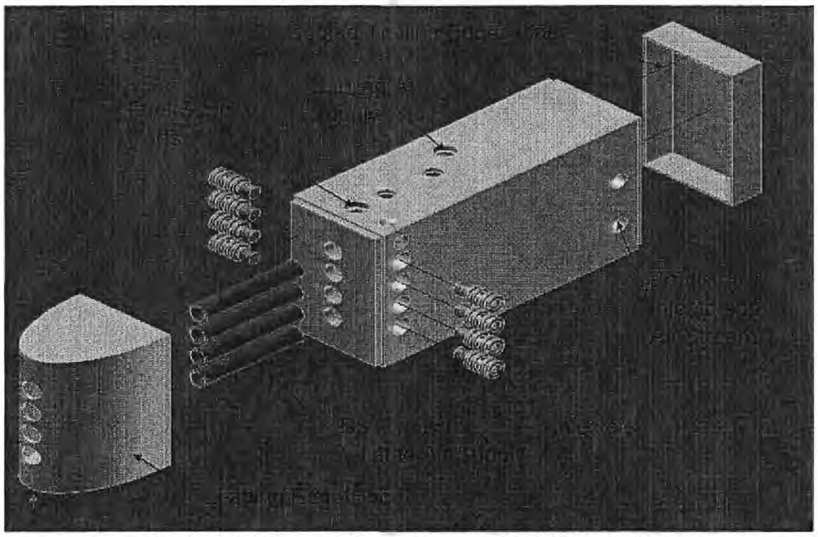

Figure 2: Exploded View of Baseline CFIS Flameholder Assembly

3. Methodology

Single flameholder augmentor (SFA) tests were performed at the Georgia Tech test rig in order to determine the stability characteristics of the CFIS flameholder. Inlet air parameters such as Mach number, oxygen content, and temperature were varied in addition to performing sweeps of global afterburner equivalence ratio throughout the experiments. Furthermore, wake fuel injection configurations were changed throughout the course of experimentation in an effort to determine stability limits of various CFIS flameholder configurations.

The first flameholder configuration tested made use of both carbureted and cross-flow fuel injection due to concerns of flow blockage and vaporization difficulties if eight injectors were distributing fuel simultaneously into the carburetor channels. In this configuration, 4 cross-flow injectors and 4 CFIS injectors were implemented in such a way that only one injector was distributing fuel in each carburetor channel. The second configuration tested involved replacing the 4 cross-flow injectors with carburetor injectors so that all eight injectors were injecting into the carburetor channels. In both configurations the baseline CFIS flameholder design was implemented.

In an effort to reduce momentum of the CFIS fuel spray normal to the main vitiated air flow and provide better fuel distribution in the recirculation zone, a third flameholder configuration was manufactured and tested that would allow fuel injection through the CFIS and directly into the wake simultaneously. A schematic representing this configuration is shown in Figure 3, and a photograph of this flameholder design is shown in Figure 4. The ratio of fuel distributed through the CFIS channel exits and directly into the wake was controlled by a valve as shown in Figure 4.

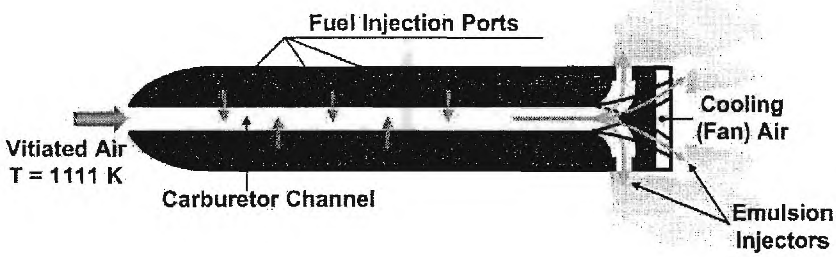

Figure 3: Conceptual Schematic of CFIS Flameholder Configuration Three

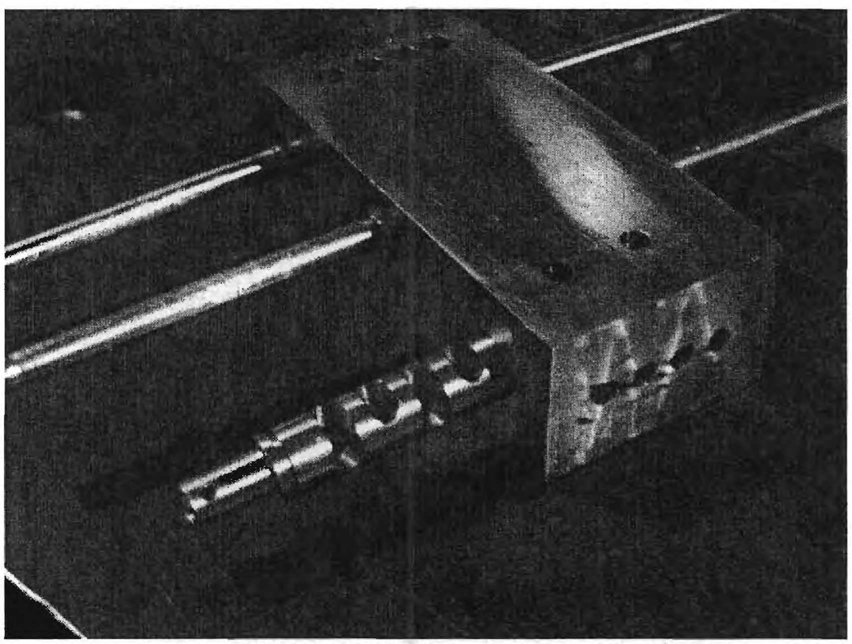

Figure 4: Photograph of CFIS Flameholder Configuration Three

A fourth fuel injection configuration was developed in which the CFIS exit channels were angled in order to reduce the momentum of the fuel-air mixture normal to the main air flow. This is the flameholder configuration that is currently being used in the SFA tests. The CFIS exits are angled 20 degrees with respect to the axis of the incoming air flow, as shown in Figure 5. In this configuration the injection channels that were previously distributing fuel directly into the wake (Configuration 3) have been plugged, as well as the insertion location for the valve so that all of the fuel-air mixture is distributed through these angled carburetor exits. Figure 6 shows a photograph detailing these modifications. A summary of all four flameholder configurations tested to date is shown in Table 1.

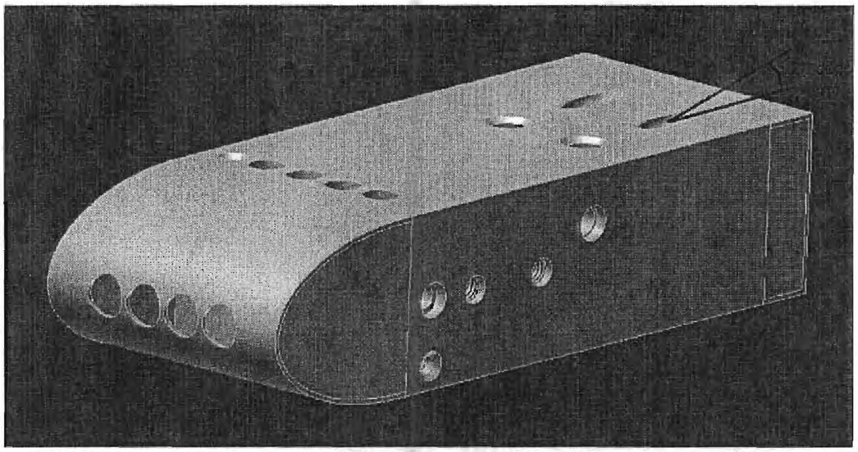

Figure 5: 3D CAD Drawing of CFIS Flameholder Configuration Four Showing Angled Carburetor Exits

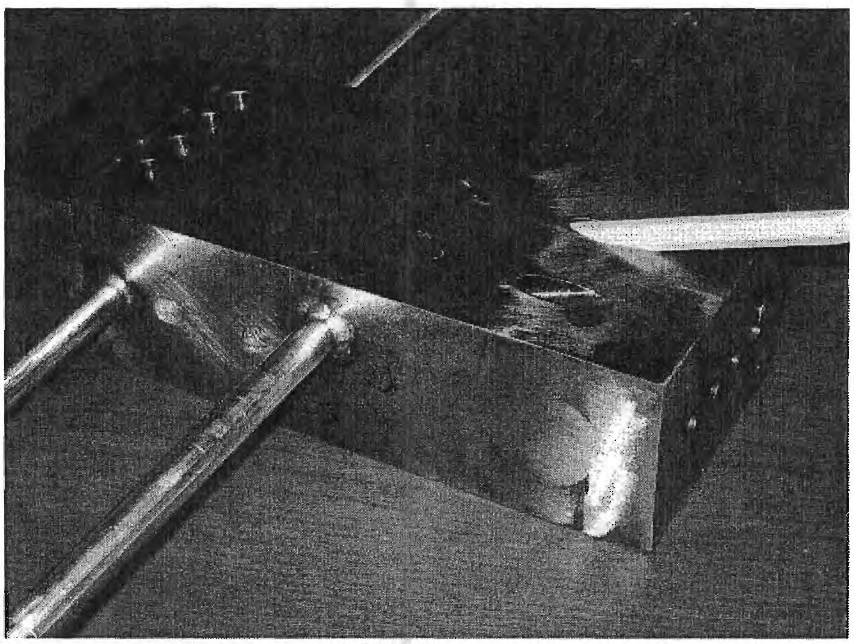

Figure 6: Photograph of CFIS Flameholder Configuration Four

Table 1: Summary of CFIS Flameholder Configurations Tested to Date

Configuration	CFIS Injectors	Cross-Flow Injectors	Wake Injection	CFIS Exit Angle (°)
1	4	4	No	90
2	8	0	No	90
3	8	0	10% to 50%	90
4	8	0	No	20

In addition to performing sweeps of operating conditions in order to determine stability limits, a Phase Doppler Particle Analysis (PDPA) was performed during the initial test of Configuration 4 to determine fuel droplet size, velocity, and volume flux from the CFIS exits and in the vane wake. Three separate two-dimensional scans were performed during the experiment. In each scan data was collected along two cross-sections with vertical axes normal to that of the main air flow, detailed in Figure 7. Data was collected just downstream of the point of injection from the CFIS channel exits and at a point 5 mm downstream of the trailing edge. The first two scans were taken without flame holding, while the third scan was performed with a stable flame being produced. Table 2 summarizes the operating conditions for each PDPA scan.

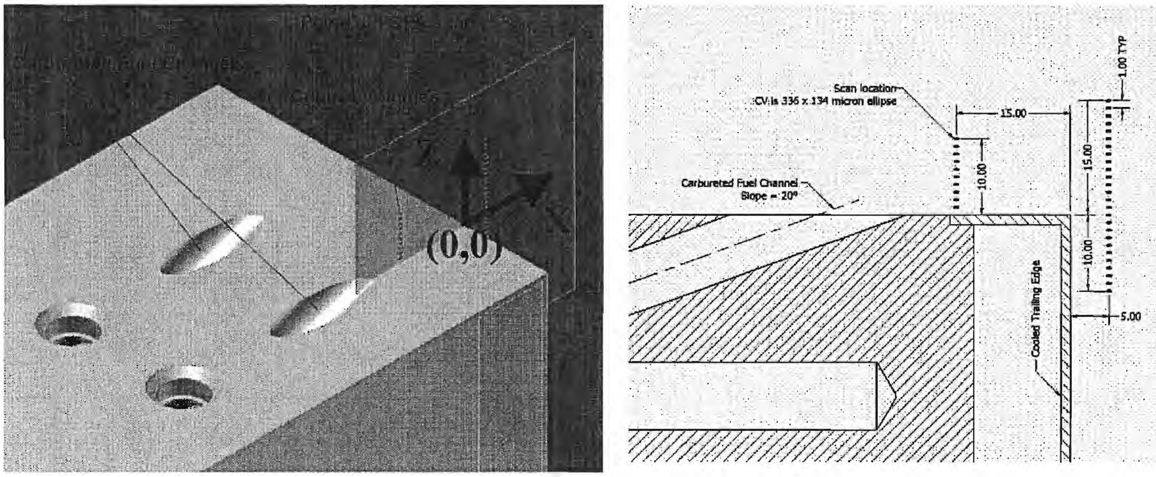

Figure 7: Schematic Detailing PDPA Scan Cross-Sections

Table 2: Summary of Operating Conditions during PDPA Scans for Experiment 4

Scan	T inlet air (°C)	Mach #	T_{AB} (°C)	$\Phi_{global, AB}$	O_2 %	Fuel Flow Rate (g/s)	Flameholding
1	348	0.20	787	0.50	14.2	13.4	no
2	348	0.20	787	0.50	14.2	13.4	no
3	344	0.19	802	0.20	14.1	5.35	yes

4. Results

Inlet air conditions and afterburner global equivalence ratio were varied during the testing of all four CFIS flameholder configurations in order to determine the stability limits of each configuration. Operating conditions and results of all four experiments are displayed in Table 3. For all four configurations stable flames were only produced at lean equivalence ratios. Flame holding above these lean conditions was only achieved with the presence of a hydrogen torch.

Table 3: Summary of Experimental Operating Conditions and Results

Date	Configuration	O2%	Ma #	T (AB) °C	Φ unassisted	Φ assisted
8/2/2007	1	13.1 - 15.2	0.21 - 0.38	720 - 860	0.20 - 0.25	0.25 - 0.55
8/3/2007	2	14.5	0.20	760	0.45	ND
8/14/2007	3	13.3 - 14.9	0.16 - 0.21	811 - 892	0.20 - 0.25	0.25 - 0.45
8/24/2007	4	14.1	0.19	802	0.20 - 0.26	0.25 - 0.65

High-definition videos of each experiment were recorded, and from these videos instantaneous images of flames produced by CFIS Flameholder Configurations 1-4 are shown in Figures 8-11, respectively. Note the corresponding operating conditions the instant each image was captured is listed in the caption. In addition to the flame being produced one can observe the fuel-air spray emanating from the photograph of the second configuration.

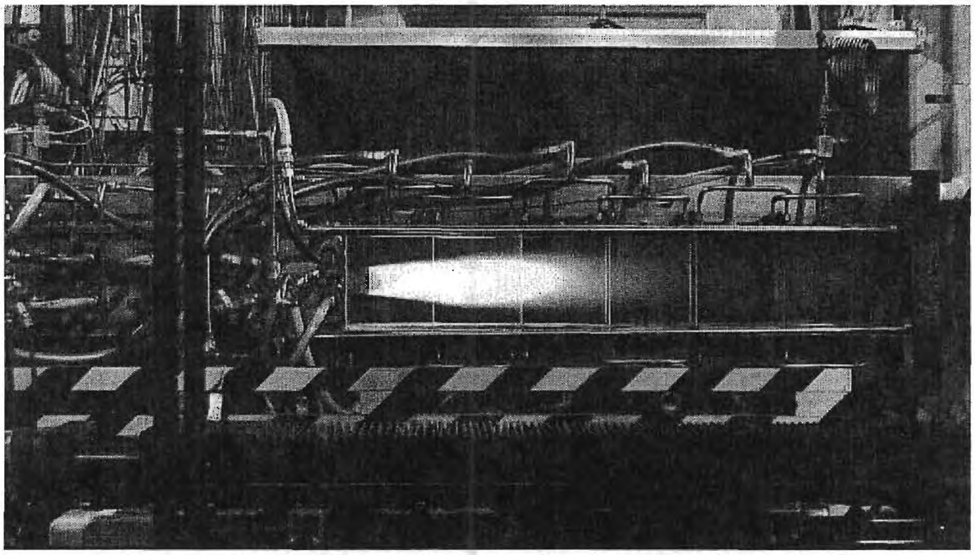

Figure 8: Configuration 1 at $\Phi = 0.23$ and Ma = 0.37

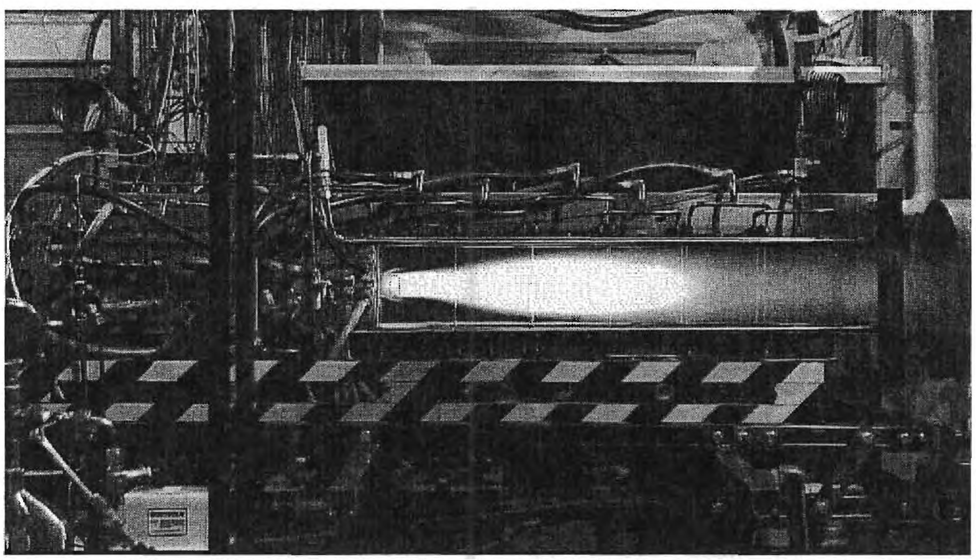

Figure 9: Configuration 2 at $\Phi = 0.45$ and Ma = 0.37

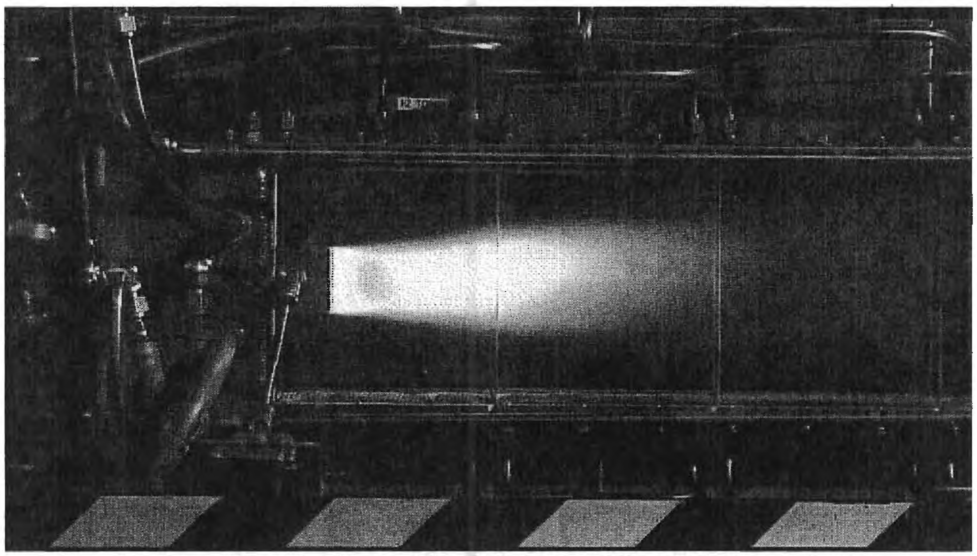

Figure 10: Configuration 3 at $\Phi = 0.15$ and Ma = 0.21

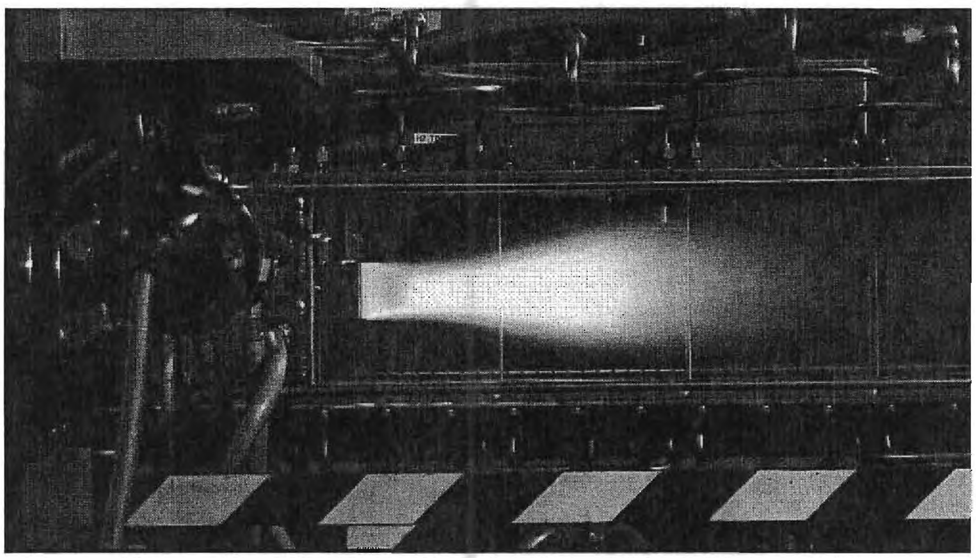

Figure 11: Configuration 4 at $\Phi = 0.20$ and Ma = 0.19

In Figures 8-11, the flames produced by each configuration appear to be relatively short when compared to flames produced by vanes incorporating conventional cross flow injectors. Figures 12 and 13 compare flame lengths produced by a conventional vane configuration and the CFIS design (Configuration 1), respectively. The operating conditions were the same for both images. The conventional vane configuration employed eight cross-flow injectors with the same diameters used in the CFIS design. From these images one can observe that the flame length produced by the conventional flameholder is 20% longer than that of the CFIS design.

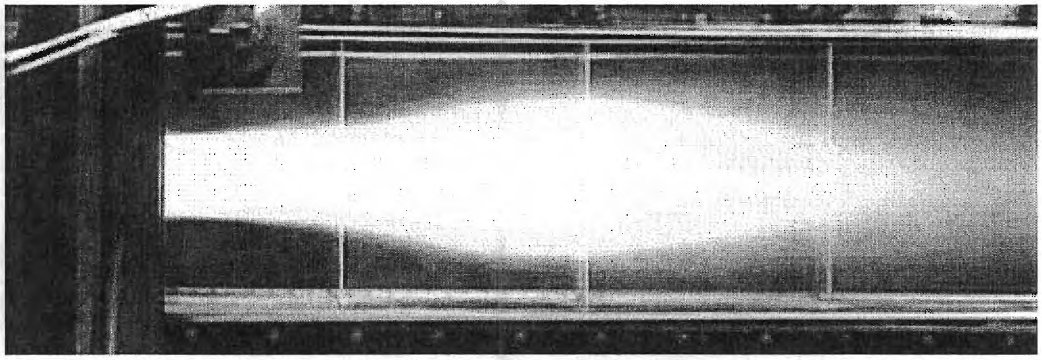

Figure 12: Flame Produced by Conventional Flameholder at $\Phi = 0.22$, Ma = 0.37

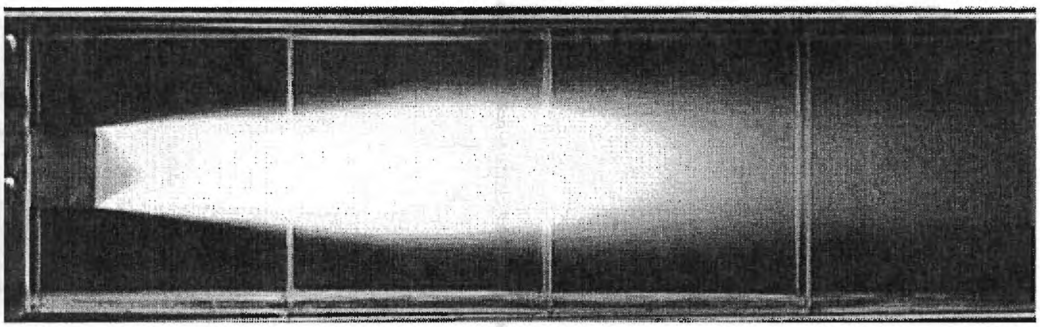

Figure 13: Flame Produced by CFIS Flameholder at $\Phi = 0.22$, Ma = 0.37

All four configurations of the CFIS flameholder are able to operate stably at lean operating conditions and without major acoustic disturbances. This is an advantage when compared to experimental results of the vane flameholder employing conventional cross-flow injection, which demonstrated "rambling" (f = 200 Hz) while operating at $\Phi < 0.55$. However stability limits of the CFIS flameholder need to be increased to include richer operating conditions in order to optimize flameholder performance. Figure 14 shows an image of the CFIS flameholder operating at equivalence ratios higher than its stability limitations in which flame holding was only achieved with the assistance of a hydrogen torch.

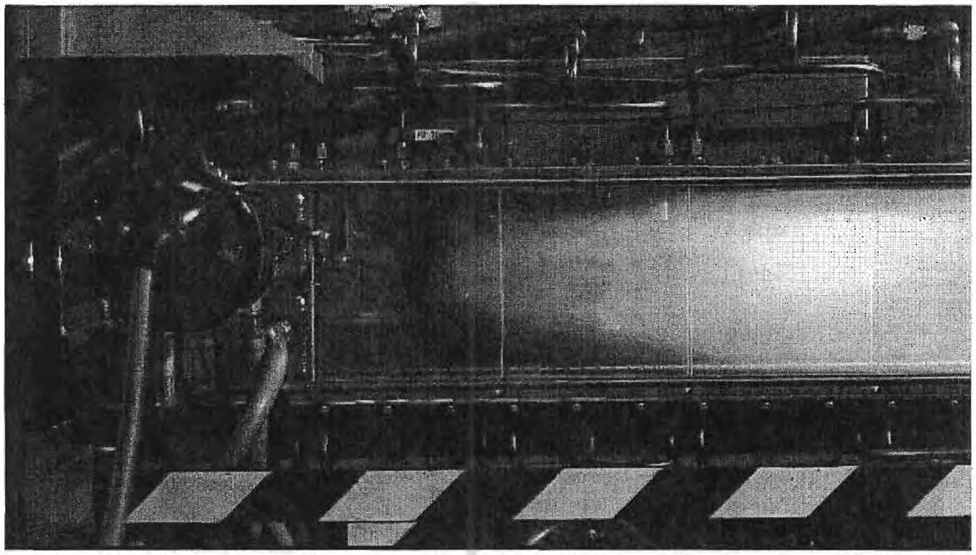

Figure 14: CFIS Flameholder Configuration 4 Operating at $\Phi > 0.25$ assisted by Hydrogen Torch

In order to help determine reasons for limited stability, two-dimensional PDPA scans were performed during the experimentation of CFIS Flameholder Configuration 4, the results of which are displayed in Figures 15 – 17. Each figure represents the PDPA data collected without flame holding, with operating conditions shown previously in Table 2. In all three figures the point z = 0 corresponds to the flameholder top surface and x = 0 the trailing edge, as previously shown in Figure 7. Figure 15 shows fuel droplet velocity distribution both in the plane of injection and in the vane wake. In the injection plane the velocity distribution is parabolic in shape, with velocity components reaching maximums of 150 m/s in the horizontal (x) direction and 30 m/s in the vertical (z) direction. These velocity components are both zero along the top surface (z = 0) of the flameholder. For the scan location in the wake, the horizontal droplet velocity component becomes negative at a point 6 mm below the flameholder surface, indicating recirculation in this region. The vertical velocity component is slightly negative in the region between z = +5 mm and z = -5 mm, also an indication of recirculation.

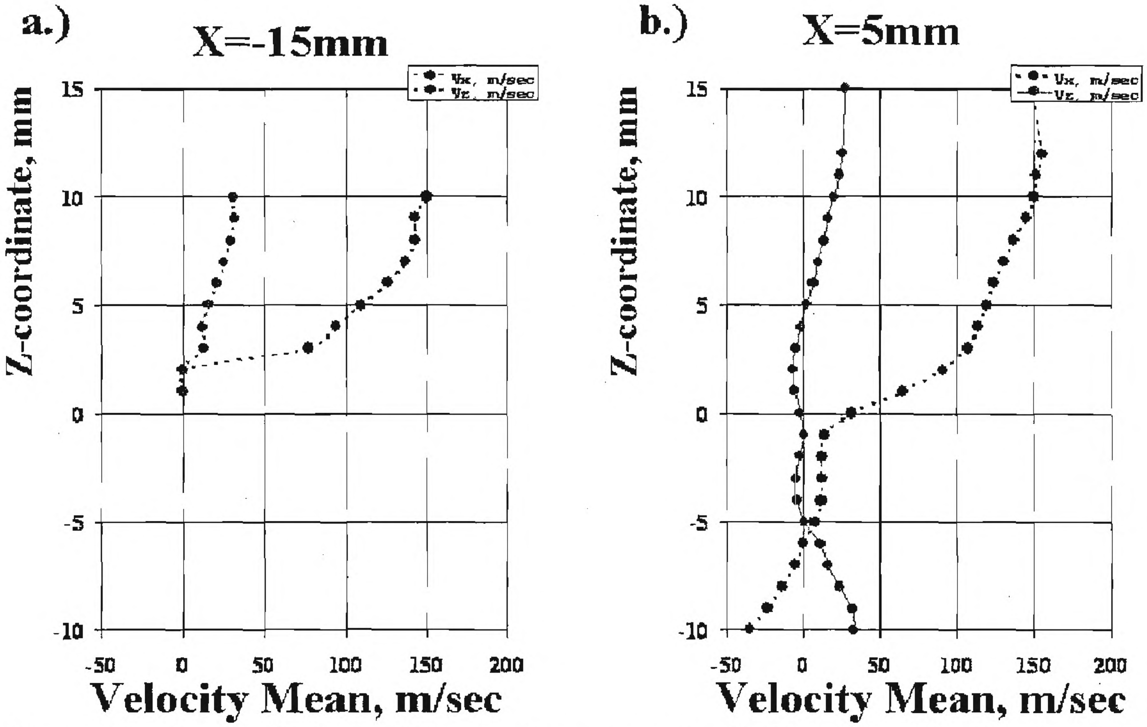

Figure 15: Droplet Velocity Distribution across the CFIS spray; a) in the plane of injection and b) in a wake of the vane.

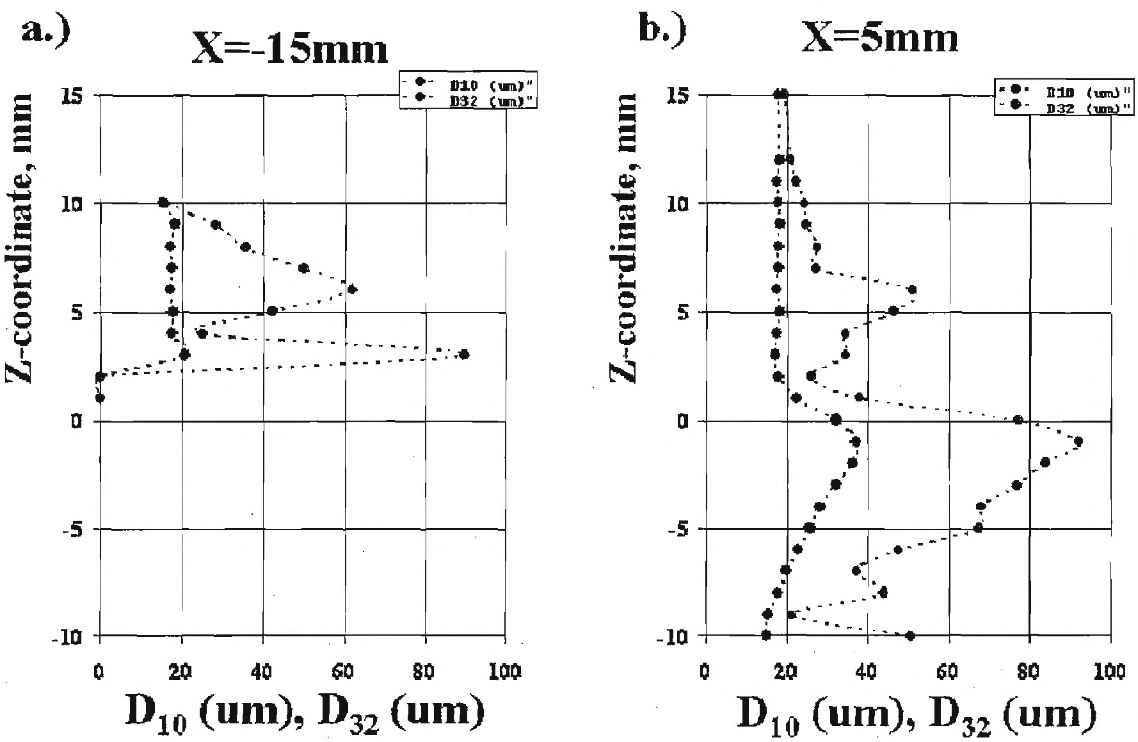

Figure 16: Droplet Size Distribution across the CFIS spray; a) in the plane of injection and b) in a wake of the vane.

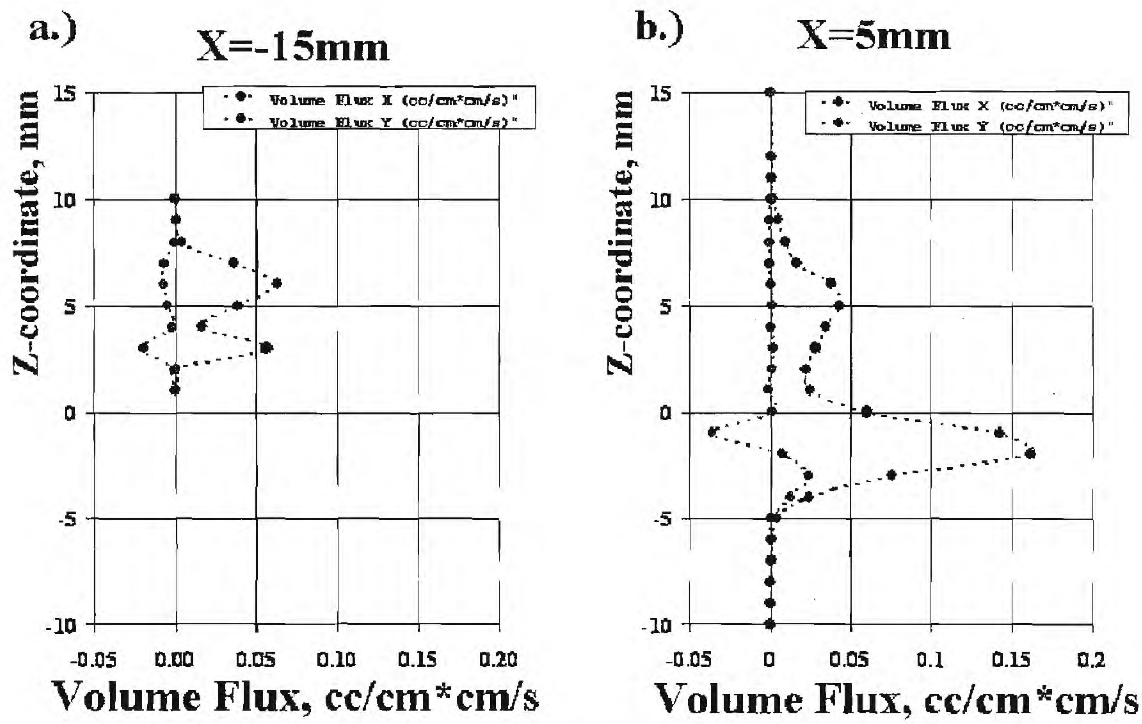

Figure 17: Volume Flux Distribution across the CFIS Spray; a) in the plane of injection and b) in a wake of the vane.

Figure 16 displays fuel droplet diameter distributions in both scan locations. The arithmetic mean diameter (D_{10}) is approximately 20 microns throughout the plane of injection as well as above the vane in its wake. These results reveal generally good aerodynamic break up and atomization of the fuel spray in the CFIS channels prior to injection. However Sauter Mean Diameter (SMD - D_{32}) distribution measured in the injection plane reveals two maximums (z = 3mm and z = 6 mm), which suggests the presence of liquid films breaking up from the surfaces of the CFIS exits, forming small amounts of large droplets on the outermost parts of the fuel-air mixture spray. Mean diameters (D_{10} and D_{32}) measured in a wake of the vane reveal one maximum on the D_{10} plot approximately 1.5mm below the top surface of the vane and two maximums on the D_{32} plot at positions z = 6mm and -1.5mm. This data suggests that small amounts of large droplets formed by film break up from the surfaces of CFIS channels propagate towards the wake plane. In addition, significant amounts of large droplets (as evident by maximums on both D_{10} and D_{32} plots) are formed by disintegration of the liquid film, which breaks up from the surface of the vane as a result of the low spray angle.

Figure 17 shows plots of volume flux distribution across the spray at both scan locations (injection plane and wake of the vane). As indicated by the graphs the same maxima mentioned above for D_{32} are occurring in the same locations in these plots as well, further supporting the idea that liquid films of fuel are developing on the surfaces. In addition, this figure shows negligible volume flux of fuel droplets at distances greater than 5 mm below the top surface of the flameholder, indicating poor entrainment of fuel in the wake.

5. Discussion of Results

All four CFIS Flameholder configurations tested to date have been able to produce stable flames unassisted by the hydrogen torch only at lean operating conditions. There are several factors believed to be contributing to these results. In all four configurations the momentum flux ratio of the fuel-air mixture emanating from the CFIS channels to the main air flow does not appear to be optimized (too high for Configurations 1 – 3 and too low for Configuration 4), resulting in poor fuel entrainment in the recirculation zone. Initial PDPA scans for Configuration 4 measured zero volume flux of droplets in the center of the vane wake immediately downstream of the trailing edge.

Configuration 3 allowed the simultaneous distribution of fuel through the CFIS channel exits normal to the main air flow and directly into the wake in an effort to distribute fuel in the recirculation zone more effectively. This method was successful at lean operating conditions (0.20 – 0.25), however at higher equivalence ratios the fuel-air spray exiting the trailing edge in an axial direction into the wake appeared to be disturbing the recirculation zone, "pushing off" the vortices that are believed to control stability.

An encouraging result of the PDPA scans is the fuel droplet size distribution emanating from the CFIS exits and into the recirculation zone. The arithmetic mean diameter of the droplets emanating from the CFIS channel exits is approximately 20 microns. These small droplet diameters are indicators of generally good aerodynamic breakup of the fuel spray injected into the carburetor channels due to the high temperature and velocity of the inlet air. These fuel droplet sizes are in agreement with those predicted to occur based on high Weber number values (~300) at the injection site into the carburetor channels.

However, the PDPA results (mainly Figure 17) suggest that there is not enough fuel volume present in the vane wake to support combustion. In addition, local maxima of fuel droplet diameter and volume flux shown in Figures 16 and 17 are believed to be the result of liquid films of fuel collecting along the outer surface of the CFIS exits and producing large droplets in the locations corresponding to these maxima. Visual examination of the flameholder after the test indicating small soot formation along the top surface of the flameholder near these exits further supports this theory.

6. Conclusion and Recommendations

- SFA tests were performed on four different CFIS Flameholder fuel injection configurations in order to determine stability limits of each design. Unassisted flame holding was achieved at lean conditions: $\Phi = 0.20 - 0.25$ for Configurations 1, 3, and 4, and $\Phi = 0.45$ for Configuration 2. PDPA scans were taken during testing of Configuration 3, characterizing the fuel spray in the injection plane and in a wake of the vane.
- Experimentation of the CFIS flameholder revealed certain advantages of this novel injection scheme. First, fuel droplets formed in the carburetor channels are smaller ($d \sim 18\mu m$ vs. $d \sim 28\mu m$ for conventional injectors), indicating generally good aerodynamic breakup of the fuel jet. Stable flame holding was achieved at lean operation without "rambling" ($f = 200$ Hz) typically observed with conventional injectors. Finally, the flame produced by the CFIS flameholder was shorter than that of the conventional injectors.
- However stability limits of the CFIS flameholder should be significantly expanded to higher equivalence ratios. This can be achieved by optimization of the momentum ratio of the fuel spray injected from the surface of the vane into the incoming flow of vitiated air and by optimization of CFIS spray injection into the recirculation zone of the vane. Both modifications will target proper fuel placement in a wide range of equivalence ratios and eliminate large droplets resulting from liquid film on the surface of the vane.
- In future testing optical diagnostic tools will be further implemented in order to gain a better understanding of the CFIS flameholder operation. PDPA scans will measure fuel droplet size, distribution, velocity, and volume flux out of CFIS exit channels and in the recirculation zone. Static and dynamic heat release distributions will be measured with the use of a spectrometer and photomultipliers and high speed cameras.